Junction Transport in Epitaxial Film Silicon Heterojunction Solar Cells

Preprint

David L. Young, Jian V. Li, Charles W. Teplin, Paul Stradins, and Howard M. Branz

Presented at the 37th IEEE Photovoltaic Specialists Conference (PVSC 37)
Seattle, Washington
June 19-24, 2011

Conference Paper
NREL/CP-5200-50712
July 2011

Contract No. DE-AC36-08GO28308

Available electronically at http://www.osti.gov/bridge

Available for a processing fee to U.S. Department of Energy
and its contractors, in paper, from:

U.S. Department of Energy
Office of Scientific and Technical Information

P.O. Box 62
Oak Ridge, TN 37831-0062
phone: 865.576.8401
fax: 865.576.5728
email: mailto:reports@adonis.osti.gov

Available for sale to the public, in paper, from:

U.S. Department of Commerce
National Technical Information Service
5285 Port Royal Road
Springfield, VA 22161
phone: 800.553.6847
fax: 703.605.6900
email: orders@ntis.fedworld.gov
online ordering: http://www.ntis.gov/help/ordermethods.aspx

Cover Photos: (left to right) PIX 16416, PIX 17423, PIX 16560, PIX 17613, PIX 17436, PIX 17721

Printed on paper containing at least 50% wastepaper, including 10% post consumer waste.

JUNCTION TRANSPORT IN EPITAXIAL FILM SILICON HETEROJUNCTION SOLAR CELLS

David L. Young, Jian V. Li, Charles W. Teplin, Paul Stradins, and Howard M. Branz
National Renewable Energy Laboratory, Golden, CO USA

ABSTRACT

We report our progress toward low-temperature HWCVD epitaxial film silicon solar cells on inexpensive seed layers, with a focus on the junction transport physics exhibited by our devices. Heterojunctions of i/p hydrogenated amorphous Si (a-Si) on our n-type epitaxial crystal Si on n^{++} Si wafers show space-charge-region recombination, tunneling or diffusive transport depending on both epitaxial Si quality and the applied forward voltage.

INTRODUCTION

Today's commercial photovoltaic market is dominated by crystalline silicon wafer technology, however an increasing share of the market is shifting toward thin-film materials due to cost advantages in fabricating large area semiconductors. Many research groups are working on crystalline film-silicon (1-40 µm) solar cells to take advantage of the potential cost advantage, high efficiency, scientific knowledge base and marketplace inertia toward silicon-based semiconductors [1-6]. Our group has been developing a low-cost hot wire chemical vapor (HWCVD) epitaxial growth technique to form high efficiency epitaxial film silicon solar cells at temperatures between 620 and 830°C on inexpensive substrates coated in crystalline seed layers [7-10]. 2-µm-thick devices grown on heavily doped wafers have shown V_{oc} values as high as 630 mV with fill factors of 78%. Devices grown on seed layers (both hetero- and homo-epitaxy) with no Si wafer exhibit device parameters that exceed those of fine-grained polysilicon devices on display glass.

These high voltages indicate high quality epitaxial material with effective minority carrier diffusion length, Leff, more than 3 times the absorber thickness.[7] However, our epitaxial films have threading dislocation densities in the 10^4 – 10^6 cm^{-2} range (imaged by electron-beam induced current) and crystalline pit and tower structures on the surface of the films at densities <10^4 cm^{-2} [9, 11] (imaged by scanning electron microscopy). The effect of these electronic and crystallographic structures can be significant [9, 11] and yet the high V_{oc} values our a-Si/c-Si heterojunction cells demand a closer look and analysis. The question addressed here is whether devices made from our low-temperature epitaxial films, despite the dislocation, pits and towers, can operate with similar transport physics as wafer-based heterojunction devices [12]. In other words, can our films form electronically clean enough interfaces and provide long enough bulk minority carrier lifetimes to allow tunneling and diffusive transport across the interface rather than voltage-killing recombination in the bulk [12].

In this contribution, we will compare the device physics of our heterojunction solar cells with that of wafer-based a-Si/c-Si heterojunction solar cells. Our study relies on analysis of temperature dependent dark current density vs voltage (JV(T)) measurements. The transport mechanisms measured in our best film-silicon devices are similar to those of the wafer-based a-Si/c-Si heterojunction solar cells, but further improvement of the Si epitaxy is needed to improve V_{oc} values to the 650 mV range.

EXPERIMENT

Epitaxial films are grown by HWCVD using a gas mixture of SiH_4, H_2, and PH_3 over a temperature range from 650 to 830 ˚C. Details of the film growth can be found elsewhere [7, 9, 13]. Films are grown on either heavily doped ($2x10^{19}$ cm^{-3}), RCA cleaned, Si:As wafers or on a variety of substrates coated with proprietary seed layers to promote epitaxial silicon growth. Seed substrates are glass, ceramic or metal foils. Heterojunction formation (~5 nm of intrinsic a-Si followed by ~15 nm of p-type a-Si:B) is done in a separate HWCVD deposition chamber after a 4% HF etch. Next, a 700 nm thick layer of In_2O_3:Sn is deposited by reactive evaporation to provide a transparent conducting layer and a top contact. Small area (0.05 cm^2) round mesa devices are isolated by wet and dry chemical techniques. Back contacts are formed either to the highly conducting wafer or to a grown-in, heavily doped back surface field layer (See reference [7] for details).

Epi/a-Si Device	Voc (mV)	Jsc (mA/cm²) {No light trapping}	FF (%)
1	627	12.43	74.98
2	600	14.1	75.4
3	570	15.3	72.5
4	555	17.7	68.6
5	555	11.7	67.2

Table 1, Device parameters.

Measurements of light current density vs voltage are done with a calibrated AM1.5 solar simulator to give device operating parameters. JV(T) measurements are made between 77 K – 350 K, at ~10°C steps, with a Linkam Scientific cryostat and a Keithley 6517B electrometer. DLTS measurements are made with custom equipment.

RESULTS AND DISCUSSION

Samples of different quality were selected for this study to determine the main junction transport mechanism responsible for limiting V_{oc} in our films. Table 1 shows device parameters for these samples. Note that devices 1-4 have V_{oc} ranging from 555 to 627 mV while the difference between devices 4 and 5 is the J_{sc} value.

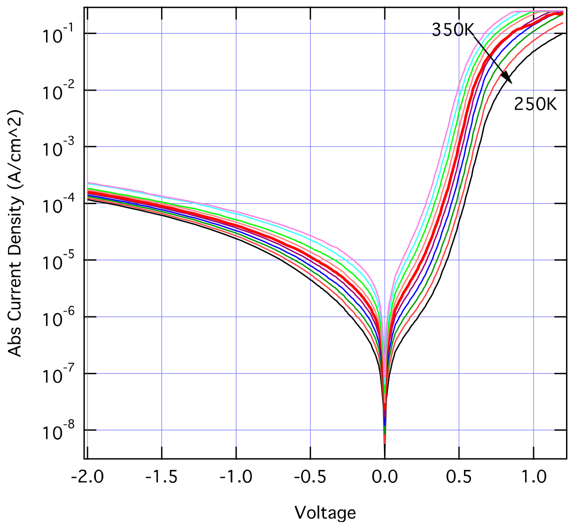

Figure 1. Temperature dependent dark current density vs voltage for device 1. Currents decrease monotonically as measurement T decreases as indicated by the arrow.

Device 1 reached the highest Voc through a hydrogen passivation treatment that will be described elsewhere. Here, we will show detailed data for Device 2, with V_{oc} = 600 mV, and compare them to key results and conclusions for the other devices. Figure 1 shows dark JV(T) data for Device 2 over the temperature range of 250 – 350 K and voltage range of -2 to 1.2 Volts.

The forward bias data of Fig. 1 can be fit with a simplified diode relationship

$$J = J_o \exp[AV] \qquad [1]$$

where

$$A = \frac{q}{nkT} \qquad [2]$$

for both diffusion and space-charge-region recombination (SCRR) models. Here, *k* is Boltzmann's constant, *T* is the measurement temperature, *n* is the diode ideality factor and *q* is the elementary charge. However, if transport is instead governed by tunneling, *A* becomes a temperature-independent constant. The pre-exponential factor J_o can be described by

$$J_o \propto \exp\left(-\frac{\Delta E_a}{kT}\right) \qquad [3]$$

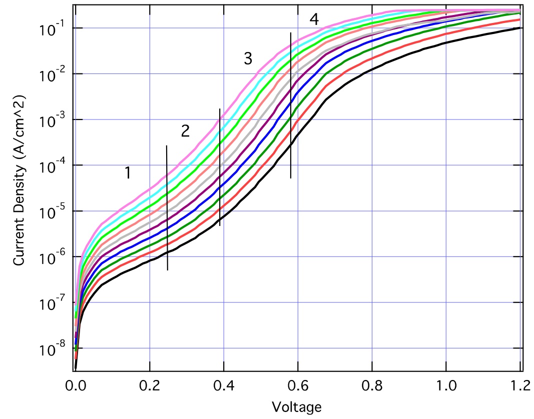

Figure 2 Forward bias temperature dependent dark current density vs voltages for device 1 showing the 4 bias regions discussed in the text. [I'd add the T arrow again]

where ΔE_a is an activation energy associated with the rate limiting recombination process [14]. Analysis of the forward bias data in Fig. 1 reveals four voltage regions characterized by a significant change in slope (different *A* values in Eq. 1) or some curvature. These regions, identified in Figure 2, each indicate a change in transport mechanism. A 2-parameter fit of the forward bias data of Fig. 2 to Eq. 1 gives the temperature dependence of the *A* factor (see Fig. 3) and J_o (see Fig.4) in voltage regions 1-3. In contrast, region 4 shows the $J \sim V^2$ dependence characteristic of space-charge-limited transport in high forward bias [15].

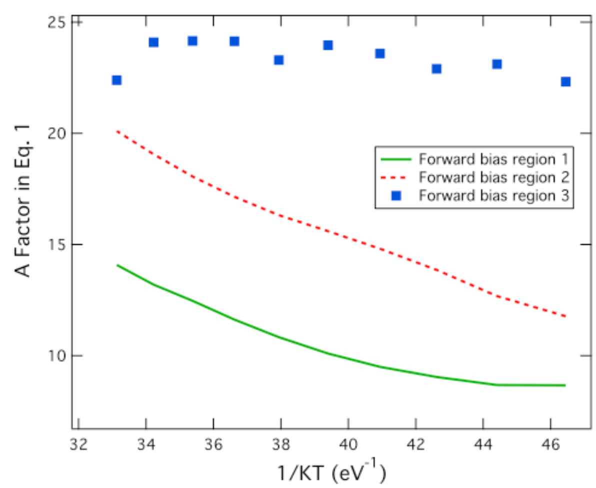

Figure 3. *A* value (Eq. 1) vs 1/kT for different bias regions from device 1.

Fig. 3 clearly shows that *A* depends strongly on T in regions 1 - 2 but is nearly T-independent in Region 3.
In regions 1 and 2, Eqn. (2) yields *n* values above 2, consistent with a space-charge-region recombination (SCRR) mechanism [16]. In Region 3, the *A* factor is

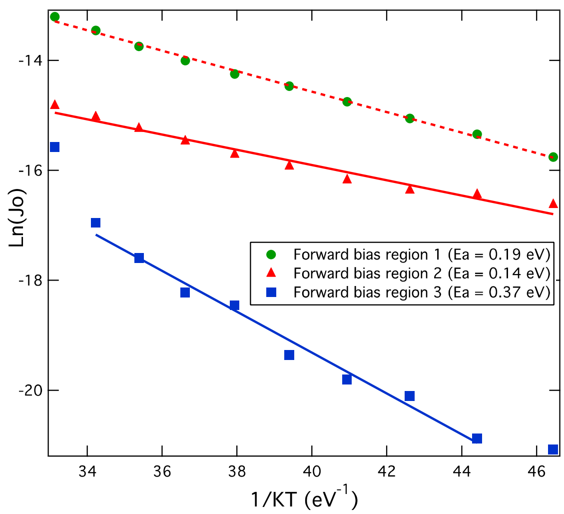

Figure 4. Ln(J_o) vs 1/kT for different bias regions from device 1. E_a values (Eq. 3) are shown in the legend.

nearly constant over the temperature range measured indicating tunneling transport as the rate limiting step [15].

Figure 4 shows *ln(J_o)* vs. *1/kT*, that we use to find the slope E_a, which is the transport activation energy according to Eq. (3). Bias regions 1 and 2 give lower E_a values (0.19 eV and 0.14 eV, respectively), while E_a in region 3 is much higher at 0.37 eV. The lack of T-dependence of A in Region 3 is consistent with the multitunneling capture-emission model of Matsuura et al [14]. The activation energy of Jo in Region 3 is consistent with the conductivity activation energy in the doped p-type a-Si:B layer (~ 0.4 eV) as noted elsewhere [12, 14].

Device	Type	Voc (mV)	Transport at low bias	Transport at high bias
1	Epi/a-Si	627	Tunneling (0.34 eV)	Diffusion (E_{act} = 0.92 eV)
2	Epi/a-Si	600	SCR (E_{act} = 0.14eV)	Tunneling (E_{act} = 0.37 eV)
3	Epi/a-Si	570	Tunneling? (E_{act} = 0.33 eV)	SCR (E_{act} = 0.49 eV) mid gap
4	Epi/a-Si	555	Tunneling (E_{act} = 0.37 eV)	SCR (E_{act} = 0.53 eV) mid gap
5	Epi/a-Si	555	SCR (E_{act} = 0.31 eV)	SCR (E_{act} = 0.33 eV)
6	Sanyo HIT cell (from Taguchi et al. (2008)	710	Tunneling (E_{act} =0.41 eV)	Diffusion (E_{act} 1.13 eV)

Table 2 Identified transport mechanisms and associated E_a for low and high forward bias regions.

From the data of Figures 1- 4, it is clear that the operating transport mechanism within Device 2 shifts with increasing forward bias from an SCRR capture/emission process to/from increasing shallow defects, followed by an abrupt change to tunneling-like behavior as the forward bias approaches V_{oc}. The E_a ~0.4 value of J_o in the tunneling region suggests [12] that the dominate dark current arises from an electron in the conduction band of the n-type epi c-Si tunneling through states in the i-a-Si layer, separated by energy < kT, to recombine with a hole from the a-Si:B layer. The hole transport through the p-layer is presumably the rate-limiting step.

Similar analysis of dark JV(T) data were completed for devices 1-5. The results from these devices are shown in Table 2. At low bias (typically less than 0.4 V) the lower-voltage devices 3 and 4 show tunneling behavior with similar E_a values to that of Device 2. However, at high bias (greater than 0.4 V) the *A* value in Eq. 1 becomes temperature *dependent* with an *n* value greater than 2 and an E_a value around 0.5 eV. These data indicate SCR recombination to a mid-gap level in the c-Si epitaxy layer near the operating voltage of the device. The worst-performing Device 5 showed SCR recombination with E_a ~ 0.3 eV across all forward biases. No tunneling-like transport was observed for this sample. It should be noted that device 5 showed a mid-gap minority carrier trap by DLTS. The origin of this trap is not yet known.

Device 1, with the highest Voc of 627 mV, has very different transport behavior with increasing forward bias compared to the other epi/a-Si devices. At low bias, it shows tunneling transport with an activation energy of 0.34 eV. As forward bias increases, however, the A value becomes temperature dependent with an activation energy for J_o of 0.92 eV and an n values less than 2. These values point toward diffusive transport of electrons over the heterojunction barrier rather than tunneling or SCRR in the base.

For perspective on the data of Table 2 we compare our data to a wafer-based heterojunction solar cell with V_{oc} > 710 mV fabricated by Sanyo [12]. From Table 2, we see that at low bias, the Sanyo HIT cell exhibits tunneling transport with an E_a of 0.41 eV. However, above about 0.4 V forward bias the Sanyo device switches to *diffusive* transport (*n*=1.2) with an E_a of 1.13 eV – the bandgap of the c-Si wafer absorber layer. This very significant change – apparently an optimized transport mechanism, allows the Sanyo device to have record high V_{oc} values. The Sanyo HIT cell acts like a diffused junction device near the maximum power point, but benefits from the band offsets between crystal and amorphous Si to increase V_{oc}.

Our epi/a-Si Device 1 shares the Sanyo cell's transport regimes despite having dislocations and crystallographic defects. From Table 2 we see that increasing Voc in our devices is accompanied by a dark current transport mechanism shift from SCRR recombination to tunneling and finally to diffusion over the junction barriers. The particular transport reveals much about the bulk and surface quality. Device 2 is limited by tunneling at the interface, however, Device 1 reached diffusive transport by the addition of a hydrogen passivation processing step that also increased the voltage.

CONCLUSION

Our study of c-Si/a-Si junction physics on low-temperature, HWCVD epitaxial films by dark JV(T) data indicate that space-charge-region recombination and tunneling are the main transport mechanisms operating in devices with V_{oc} < 600 mV. Devices that are hydrogen passivated prior to growth of the c-Si/a-Si heterojunction show diffusive transport over the junction barrier which allows V_{oc} values as high as 630 mV.

ACKNOWLEDGEMENT

We thank Falah Hasoon, Russell Bauer, Lorenzo Roybal, Kirstin Alberi, Max Shub, Harvey Guthrey and Vincenzo LaSalvia for assistance in sample preparation and Richard Crandall for helpful discussions. This work was supported by the U.S. Department of Energy under Contract No. DE-AC36-08-GO28308 with the National Renewable Energy Laboratory.

REFERENCES

[1] Gestel, D.V., M. Chahal, P.C.V.d. Wilt, Y. Qiu, I. Gordon, J.S. Im, and J. Poortmans, *Thin-film polycrystalline silicon solar cells with low intragrain defect density made via laser crystallization and epitaxial growth*, in *IEEE PVSC 36*, IEEE, Editor. 2010, IEEE: Honalulu, Hawaii.

[2] Wagner, T.A., L. Oberbeck, and R.B. Bergmann, "*Low temperature epitaxial silicon films deposited by ion-assisted deposition".* Materials Science and Engineering B, **89**(1-3) 2002, p. 319.

[3] Nieuwenhuysen, K.V., M.R. Payo, I. Kuzma-Filipek, J.V. Hoeymissen, G. Beaucarne, and J. Poortmans, "*Epitaxially grown emitters for thin film silicon solar cells result in 16% efficiency".* Thin Solid Films, **518** 2110, p. S80.

[4] Gordon, I., S. Vallon, A. Mayolet, G. Beaucarne, and J. Poortmans, "*Thin-Film Monocrystalline-silicon solar cells made by a seed layer approach on glass-ceramic substrates".* Solar Energy Materials & Solar Cells, **94** 2010, p. 381.

[5] Dogan, P., E. Rudigier, F. Fenske, K.Y. Lee, B. Gorka, B. Rau, E. Conrad, and S. Gall, "*Structural and electrical properties of epitaxial Si layers prepared by E-beam evaporation".* Thin Solid Films, **516** 2008, p. 6989.

[6] Green, M.A., P.A. Basore, N. Chang, D. Clugston, R. Egan, R. Evans, D. Hogg, S. Jarnason, M. Keevers, P. Lasswell, J. O'Sullivan, U. Schubert, A. Turner, S.R. Wenham, and T. Young, "*Crystalline silicon on glass (CSG) thin-film solar cell modules".* Solar Energy, **77** 2004, p. 857.

[7] Alberi, K., I.T. Martin, M. Shub, C.W. Teplin, Manuel J. Romero, R.C. Reedy, E. Iwaniczko, A. Duda, P. Stradins, H.M. Branz, and D.L. Young, "*Material quality requirements for efficient epitaxial film silicon solar cells".* APL, **96** 2010, p. 073502.

[8] Martin, I.T., C.W. Teplin, J.R. Doyle, H.M. Branz, and P. Stradins, "*Physics and chemistry of Hot-wire chemical vapor deposition from silane: measuring and modeling the silicon epitaxy deposition rate".* Journal of Applied Physics, **107** 2010, p. 054906.

[9] Teplin, C.W., K. Alberi, M. Shub, C. Beall, I.T. Martin, M.J. Romero, D.L. Young, R.C. Reedy, P. Stradins, and H.M. Branz, "*Mechanisms controlling the phase and dislocation density in epitaxial silicon films grown from silane below 800°C".* APL, **96** 2010, p. 201901.

[10] Branz, H.M., C.W. Teplin, M.J. Romero, I.T. Martin, Q. Wang, K. Alberi, D.L. Young, and P. Stradins, "*Hot-Wire chemcial vapor deposition of eptiaxial film crystal silicon for photovoltaics".* Thin Solid Films, **519** 2011, p. 4545

[11] Romero, M.J., K. Alberi, I.T. Martin, K.M. Jones, D.L. Young, Y. Yan, C. Teplin, M.M. Al-Jassim, P. Stradins, and H.M. Branz, "*Nanoscale measurements of local junction breakdown in epitaxial film silicon solar cells".* Applied Physics Letters, **97** 2010, p. 092107.

[12] Taguchi, M., E. Maruyama, and M. Tanaka, "*Temperature dependence of amorphous/crystalline silicon heterojunction solar cells".* Japanese Journal of Applied Physics, **47**(2) 2008, p. 814.

[13] Martin, I.T., R.C. Reedy, K. Alberi, C.W. Teplin, D.L. Young, K.M. Jones, A. Duda, C.L. Beall, M. Shub, M.J. Romero, H. Guthrey, E. Iwaniczko, H.M. Branz, and P. Stradins, "*Interface Control in Hot-wire Chemical Vapor Deposition of Epitaxial Silicon for Improved Solar Cells".* Manuscript in preparation, 2010

[14] Matsuura, H., T. Okuno, H. Okushi, and K. Tanaka, "*Electrical properties of n-amorphous/p-crystalline silicon heterojunctions".* Journal of Applied Physics, **55**(4) 1984, p. 1012.

[15] Sze, S.M. and K.K. NG, Physics of Semiconductor Devices. 3rd ed. 2007, Hoboken: John Wiley & Sons, INC. 815.

[16] Hovel, H.J., Semiconductors and semimetals,. Solar Cells, ed. R.K. Willardson and A.C. Beer. Vol. Vol. II. 1975, New York: Academic Press.